

Design and testing of a hybrid passive/active acoustic treatment for nacelle inlets

Marie-Annick Galland, Benoit Mazeaud

Centre Acoustique du LMFA, UMR CNRS 5509

Ecole Centrale de Lyon

36 avenue Guy de Collongue, 69134 Ecully Cedex, France

ABSTRACT

This paper deals with the design and testing of a hybrid acoustic treatment combining porous material properties and active control techniques, intended to reduce time-varying tones in flow-duct applications. A dedicated digital adaptive feedback control algorithm was developed to operate independently cell by cell, enabling easy subsequent increase of the liner surface. Large active panels of 54 cells were tested with pure sine waves from 850 Hz to 2 kHz for flow velocities up to Mach 0.3. Convergence was very rapid and stable for all cells. A detailed analysis of the experimental results is given, with comparisons with results for numerical simulation in the no-flow case. In agreement with predictions, active functioning was generally more effective up to 1 kHz, and the hybrid liner provided overall noise reduction that was largely independent of frequency.

1. INTRODUCTION

In recent years, noise has become a crucial issue in vehicle design, especially in the aircraft industry. Many research programs have sought to design efficient noise-reduction technologies. Conclusions often suggested that combined active/passive solutions best covered the entire frequency range of unwanted noise: passive structures are suited to reducing high frequency components, while active control technologies appear to be the only way to attenuate the low frequency components. The LMFA Center for Acoustics at the *Ecole Centrale de Lyon* (France) (ECL) has, over the last ten years, developed a new concept of acoustic absorber (Furstoss [1]; Sellen [2]), combining the passive properties of absorbent materials and active control.

The hybrid passive/active absorber concept is intended to extend the effectiveness of classical single-degree-of-freedom (SDOF) absorbers into the low frequency range by means of active control (see Fig. 1). The SDOF liner is a classical absorber for nacelle applications, comprising a honeycomb layer sandwiched between a resistive face-sheet (e.g., wire mesh) and a reflective back-sheet. The same principle is used in the hybrid

cell, but with the reflective sheet replaced by an acoustic source. At high frequencies, this actuator is blocked and therefore acts as a rigid wall. At lower frequencies, active control is used to reduce pressure on the rear face of the wire mesh, so that the system acts as a broadband equivalent of a $\lambda/4$ resonant absorber.

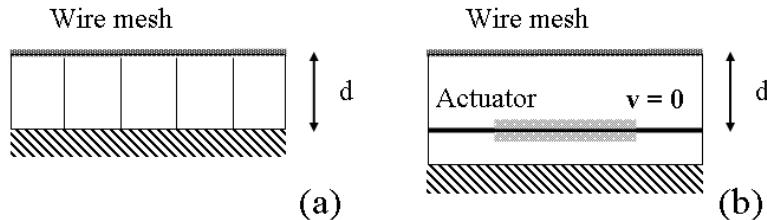


Figure 1. Design of the hybrid cell: from the classical SDOF liner (a), to the hybrid absorber cell, at high frequencies in passive mode (b) and at low frequencies in active mode (c).

A large absorber surface can be implemented by assembling several individual cells. The present paper concerns the design of such an absorber and its performance in a test-bed representative of turbo-machine applications. The basic hybrid cell is first described, with a brief summary of its main characteristics. The new test-bed is then presented in section 3. The multi-cell structure was experimentally tested for a system comprising some 50 cells in a flow-duct with pure sine waves from 850 Hz to 2 kHz for flow velocities up to Mach 0.3. Section 4 describes the hybrid panel. A multiple-input/multiple-output (MIMO) control system is necessary to reduce the pressure in each cell. Section 5 describes the dedicated decentralized algorithm developed to enlarge the active surfaces, and the controller designed for the test-bed. The performance of the control system is also analyzed in this section. The effectiveness of the hybrid liner was assessed by measuring the radiated field under various conditions. Pressure maps are analyzed in section 6. Finally, the experimental results are compared to numerical simulations, in section 7. The study was carried out under the European SILENCE(R) research program.

2. THE HYBRID PASSIVE/ACTIVE CELL

In 1953, Olson and May first suggested producing an active absorber by placing a loudspeaker behind an acoustically resistant cloth ([3]). The aim was to couple an acoustic resistance having a correctly selected value with a low active impedance, so that the overall impedance seen by the incoming wave would approximately equal the resistance of the cloth. Thus, acoustic dissipation by friction through the cloth is increased in the low frequency range. The use of active means for impedance control and sound absorption was clearly presented. However, only purely real impedances can be achieved by such an active absorber.

The case of radiation by flow ducts is examined in the present paper. In this case, the targeted impedance, defined as that leading to maximal power reduction, is no longer real. Tester [4] demonstrated that, in the case of a semi-infinite duct with a uniform flow,

the optimal resistance and optimal reactance are frequency-dependent: weak at low frequencies and increasing in absolute value with increasing frequency, the targeted reactance always remaining negative. Therefore, a hybrid passive/active absorber can be an efficient means of reducing noise in such an application: active control should kick in only at low frequencies, while at higher frequencies active control is off and the negative reactance is obtained through the air-gap behind the resistive layer. This method also offers the advantage of separating the control system from a hostile environment (e.g., the flow). However, it is not possible to reproduce exactly the optimal impedance curves with a hybrid absorber, and the radiated power is generally very sensitive to small variations in impedance value. The best compromise is obtained by combining a well-chosen resistive layer, to approach the mean value of the desired resistance, with a suitable air-gap depth behind, to fit the reactance at high frequencies.

Preliminary studies led the design of a basic hybrid cell, as shown in Fig. 2.

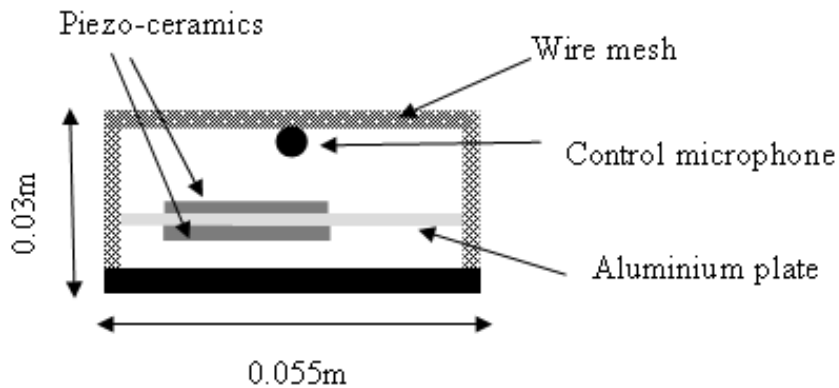


Figure 2. The basic hybrid cell

The use of a highly resistive material (wire mesh) as porous layer and a piezo-electric transducer as secondary source enables a very compact absorber less than 0.03 m thick to be implemented (Hilbrunner, [5]). The cell cross-section of 0.055 m \times 0.055 m guaranteed uniform pressure on the back face of the porous layer up to 2.5 kHz. In this way, the passive behavior corresponded to a locally reacting liner, and the pressure reduction at the error microphone in the active mode induced a significant pressure reduction over the whole rear face of the resistive sheet.

The first experiments on hybrid liners were carried out in the Matisse flow-duct at the *Ecole Centrale de Lyon* (Sellen [2]). The experimental set-up was geometrically simple (square cross-section, anechoic termination), enabling precise comparison with theoretical results. Very useful sound reduction levels were achieved for plane waves throughout the 700-2,500 Hz range, for flow velocities up to 50m/s and a treated area of

0.22m by 0.055m (four-cell system). The cut-off frequency between active and passive modes was found at 1.8 kHz, both experimentally and theoretically.

The objective of this new test campaign was to study the behavior of such treatment on a test-bed that was more representative of nacelle applications. The main changes concerned the transverse size of the duct, the treated area and the flow velocity.

3. DESCRIPTION OF THE TEST FACILITY

The test rig located in the anechoic wind tunnel of ECL is represented in Fig. 3. The test section, provided by SNECMA, was a duct of rectangular cross-section (0.24 m × 0.32 m). The two vertical walls were either rigid or featured two hybrid panels in passive or active mode. Speeds up to Mach 0.3 could be reached in this section. The ejection nozzle transformed the rectangular cross-section into a cylinder, in order to homogenize the radiated field.

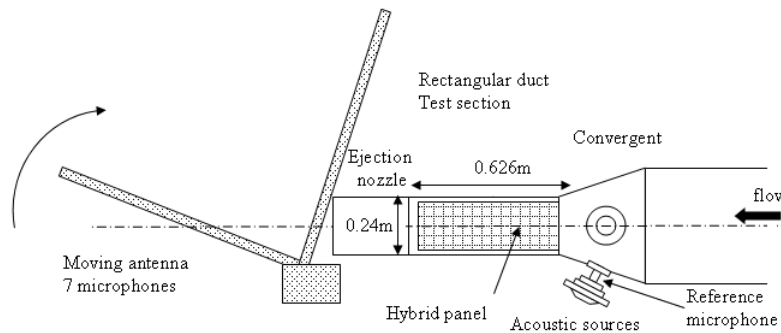


Figure 3. Lateral view of the test rig

The acoustic sources were compression chambers that allowed a high level of excitation in the rig: a reference microphone located in the coupling pipe in the vicinity of the source measured pressure levels between 135 and 145 dB. The tests were conducted with pure sine waves of different frequencies (850 Hz, 1 kHz, 1.25 kHz, 1.6 kHz and 2 kHz), using a source located either on the bottom wall or on the wall on the left of the convergent part of the rig. The tones emerged from the background level by at least 30 dB (at Mach 0.3), and more for lower Mach numbers.

A far-field antenna composed of seven B & K 1/2" 4191 microphones scanned approximately a quarter of a 1.5 m radius sphere centered on the duct exhaust (Fig.4). Pressure spectra were measured for eight angles, from 30° to 100° with respect to the duct axis, by means of an HP 3567 a multi-channel signal analyzer, for the antenna's 7 microphones and the reference microphone. A total of 56 measurement points was thereby obtained for each frequency and source position, in the cases of rigid wall and passive or active configuration of the hybrid panels. In parallel, a PXI platform using IDEAS software enabled time evolutions or spectra coming from error microphones to be recorded, in order to study the behavior of the control algorithm.

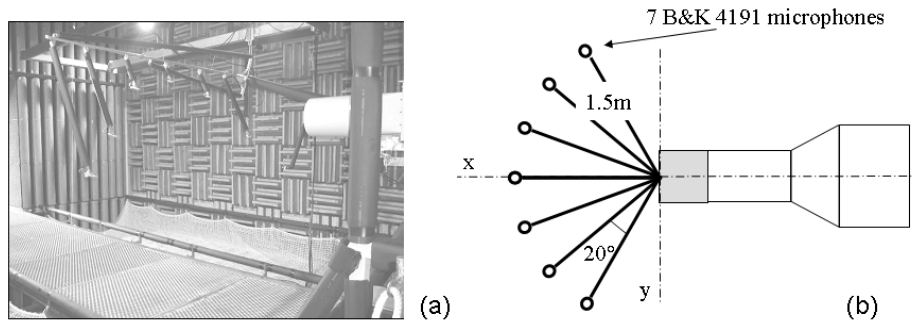


Figure 4. Microphone far-field antenna. Photo (a) and top view (b)

4. DESCRIPTION OF THE HYBRID PANELS

Two hybrid panels were manufactured by AIRBUS France and included in vertical locations in the rectangular duct, as shown in Fig.3. Each liner panel ($0.626 \text{ m} \times 0.240 \text{ m}$) featured 27 active cells (3 lines of 9 cells), as shown in Fig. 5. Special attention was paid to ensuring that the behavior of the cells remained as close as possible to the previously optimized prototype. In particular, the cell cross-section was kept at $0.055 \text{ m} \times 0.055 \text{ m}$, to guarantee uniform pressure on the back face of the porous layer in the frequency range of interest.

The porous material was selected using optimal impedance curves provided by SNECMA. Modal analysis was performed, with uniform flow under an equal energy assumption on all propagating modes, to deduce the impedance values maximizing reduction of the radiated noise. The optimal impedance values depended on the frequency and flow velocity. As previously found in the Matisse flow duct (Sellen [2]), it was not possible to reproduce the optimal impedance curves exactly with a hybrid absorber. A wire mesh with a resistance approximating Z_0 , the characteristic impedance of air, was selected as porous layer and the air gap between the wire mesh and the actuator was set at 0.02 m.

5. THE CONTROL SYSTEM

The study focused on reducing time-varying periodic noise, which is an important component of fan noise. Digital multiple-input/multiple-output (MIMO) feed-forward systems have proved to be particularly effective in controlling periodic noise. Memory requirements and computation loads, however, quickly become limiting factors for large systems, particularly when periodic noise is considered. Moreover, in the targeted final application (e.g. turbojet inlet covering), a reference signal synthesized from the engine speed may not correlate sufficiently with the perturbation for a high degree of noise reduction to be achieved. Thus, feedback control is preferable. Analog feedback controllers are unable to deal with a complex and varying environment, especially in the

case of MIMO systems. Thus, independent active cells with digital auto-adaptive feedback controllers should be the ideal system to extend the treated area in industrial applications.

We developed an original algorithm, able to achieve adaptive decentralized “cell-by-cell” feedback control to reduce time-varying tones.

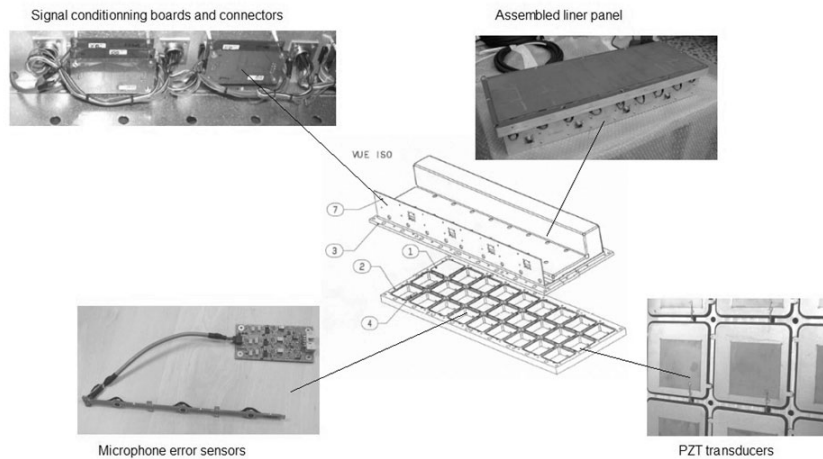


Figure 5. View of the hybrid panel components

5.1 The single-channel structure

The basic idea of such a feedback controller is to estimate the primary noise in the error sensor and to use this as the reference signal for the control filter. The use of an Internal Model Control (IMC) configuration thus allows feedforward control to be implemented through the Filtered-x LMS algorithm (see Elliott [6]). The secondary signal is estimated from the model $\hat{S}(z)$ of the secondary-path transfer function $S(z)$ and subtracted from the error signal to regenerate an estimation of the primary noise. This reference signal is then used as input by the control filter. The algorithm works similarly to the classical FXLMS algorithm for periodic noise - but with the advantage of requiring only one analog input for a single-channel system, instead of two.

5.2 The multi-channel structure

Larger surfaces are obtained by assembling several cells forming the hybrid liner. Interactions appear between cells, and cross-paths should be taken into account to synthesize an estimate of the primary signal, as in the single-channel case. This leads to a very complex structure and real-time developments are often limited for configurations requiring a large number of channels, since computation complexity and memory costs grow with the number of cross-paths. We propose a simplified version of the algorithm,

in which only the self- and main feedback produced by each cell is removed. However, while cross-contributions are ignored in this new architecture, they still exist in the physical domain and instabilities are therefore to be feared. A solution was found by filtering each reference signal by a bandpass filter located around the main tones of the primary noise. This approach leads to satisfactory control when applied to MIMO systems. Moreover, adaptive notch filters can be implemented to deal with time-varying tones, by means of a frequency-detection algorithm used to extract the tones from the signal provided by the control microphone. The whole process is described in Mazeaud [7]. This algorithm was named IMC-MDFXLMS, for IMC MIMO Diagonalized FXLMS, and the final version of its architecture is shown in Fig. 6 for one cell. The sole input required for each cell is therefore the pressure signal at the corresponding control microphone. This set-up is then reproduced for each cell, enabling the whole control system to function in parallel.

In Fig. 6, $d(n)$ represents the primary signal, $x(n)$ the reference signal (filter input) calculated from the error signal $e(n)$ (i.e., the pressure at the control microphone), and $y(n)$ the output of the control filter $W(z)$. It should be noted that off-line modeling is implemented to obtain the secondary-path estimate $\hat{S}(z)$. Although the algorithm's behavior was more sensitive to the quality of the secondary-path estimation than in the case of a purely feedforward algorithm, all the simulations and experiments performed using it showed good performance and fast tracking capabilities.

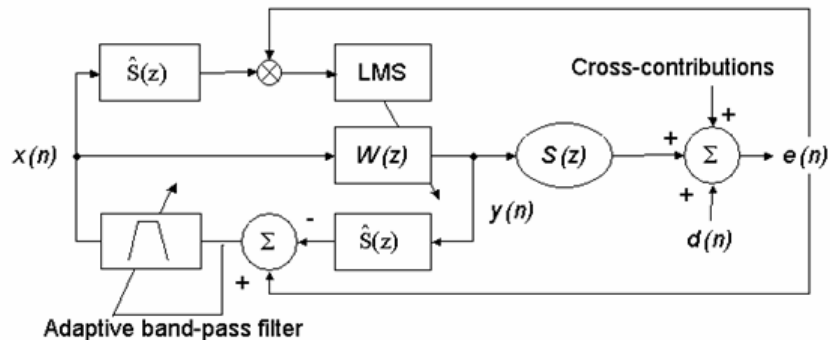


Figure 6. Detailed block diagram of the simplified multi-channel algorithm

5.3 The active control system: description and behavior

A 54-channel rack was specially developed by 01dB-Metravib (Limonest, France) as controller for the new test-bed. It featured 27 DSP cards, each controlling 2 cells. The identification procedure was first implemented for all channels in the 800-2,500 Hz frequency range, with 255-tap FIR filters. The control procedure was then run for pure tones, with 8-coefficient FIR filters using the IMC-MDFXLMS algorithm presented above. Experiments carried out with the 54-cell panels showed the bandpass filtering to achieve pressure reduction at all error sensors without instability. As seen in Fig. 7,

convergence was very rapid (less than 100 ms) and stable. Active control was not affected by the presence of flow, even with a high Mach number ($M=0.3$) as long as the tone-to-broadband-noise-ratio was adequate. The noise reduction at one control microphone is plotted in Fig. 7 as an example. This is a very interesting and promising result: the architecture of hybrid liners allowed large absorbent surfaces to be developed, and the active control was effective at a representative Mach number.

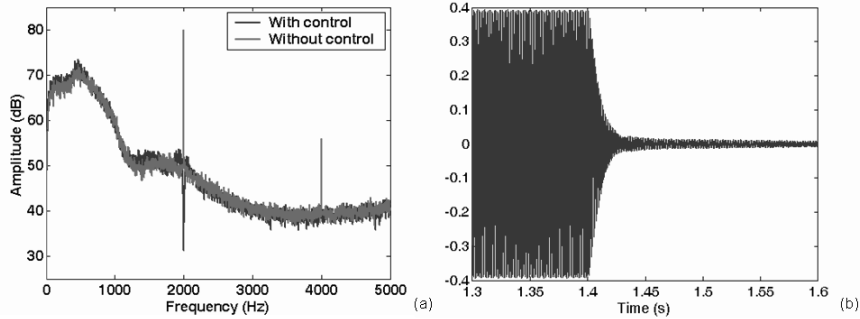


Figure 7. Measured pressure at one control microphone. Spectra with and without control for a 2 kHz pure tone and Mach 0.3 (a). Time history for a 1 kHz pure tone and Mach 0 (b).

6. EXPERIMENTAL RESULTS ON THE RADIATED PRESSURE FIELD

The results for the noise reduction obtained with the hybrid panels are presented below in the form of maps of the pressure levels measured by the antenna, for the rigid wall case and for the two passive and active modes. Only a few representative maps are presented here, to illustrate the main trends in panel behavior.

6.1 Frequency dependence

As predicted, the active mode was more effective for the low frequencies. Fig. 8 shows, by way of example, the maps for all the frequencies obtained at Mach 0.15 for the left-hand source. The terminal section of the duct is symbolized by the blue cylinder. All diagrams are plotted on the same scale, from 75 dB to 105 dB. As in this example, the liner generally provided significant noise reduction, in the active mode for the low frequencies, and in the passive mode for higher frequencies. The cut-off between active and passive functioning was experimentally located between 1 kHz and 1.25 kHz.

6.2 Influence of flow

The presence of a flow had a variable effect on the pressure field. The diagrams obtained for $M=0$, $M=0.15$ and $M=0.3$ reveal generally similar hybrid liner behavior, with effectiveness decreasing as flow velocity increases (see, for example, Fig. 9 obtained at 850 Hz with the left-hand source). The commutation frequency between

active and passive functioning did not vary. However, in the case of $M=0.3$, the active and passive functionings exhibited quite similar behavior. Both attenuations and frequency evolutions revealed similar performance at this high Mach number for the two source locations.

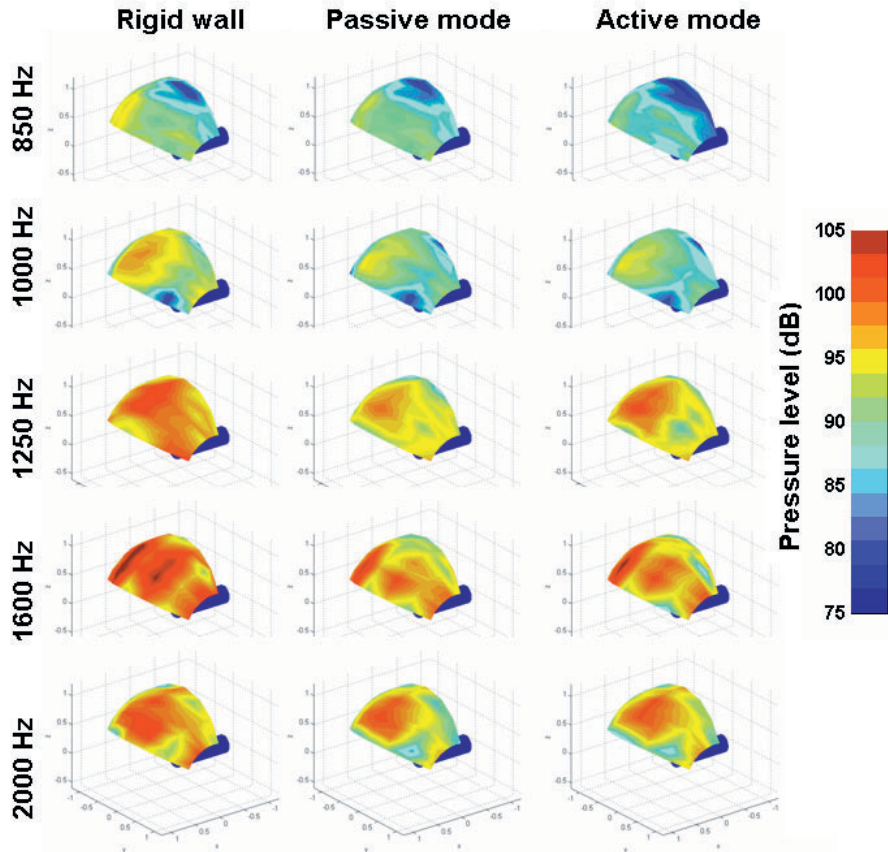


Figure 8. Pressure field measured on the antenna at Mach 0.15. The source is located on the left

6.3 Source position

Attenuation seemed to be generally more substantial when the source was located on the left. The frequency evolutions were the same overall, but with greater noise reduction in this case. Indeed, in this configuration, rays directly impinged on the liner located on the right. Further reflections eventually occurred on the opposite liner and, finally, the radiated power was more strongly reduced. When noise was produced by the

lower source, rays impinged the two liners at a more grazing incidence and the reduction was therefore less. The pressure field measured at the antenna at 1 kHz for Mach 0.15 is shown in figure 10 to illustrate this observation. In this case, active control was more relevant to increasing both the area and degree of noise reduction. However, the pressure field was not measured in the half-space under the flow, and no definite conclusion can be drawn.

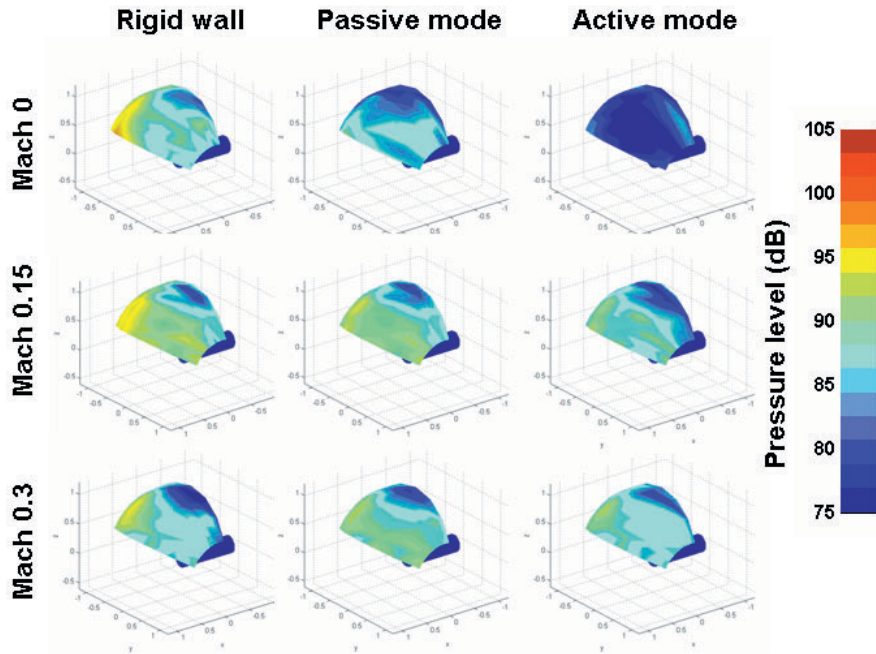


Figure 9. Pressure field measured on the antenna at 850 Hz for different Mach numbers. The source is located on the left

6.4 Radiated power. Insertion Loss

Insertion loss could be estimated from pressure measurement only in the case of the left-hand source. The symmetry in the pressure field between the upper and lower parts of the ejection nozzle allowed the radiated power to be determined. The insertion loss, defined as the difference in radiated power with and without treatment, is plotted on Fig. 11 for Mach 0.15. The hybrid functioning was once more validated, with a cut-off frequency experimentally located at 1.4 kHz in this case.

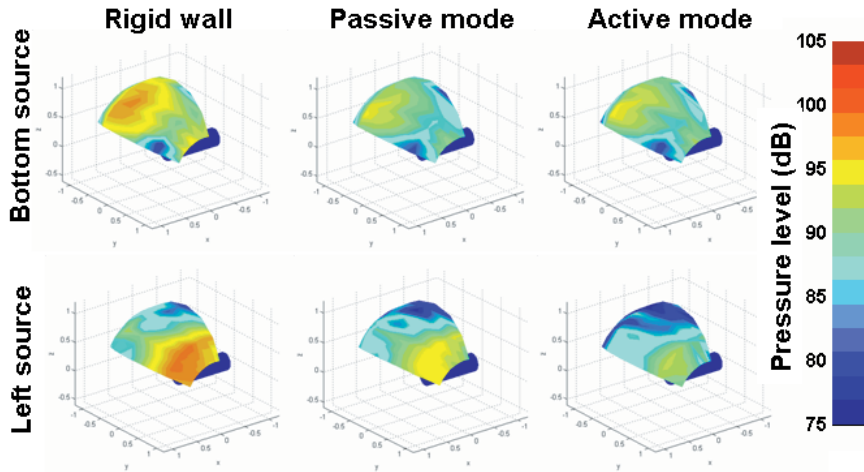


Figure 10. Pressure field measured on the antenna at 1 kHz for the two source positions. The Mach number is 0.15

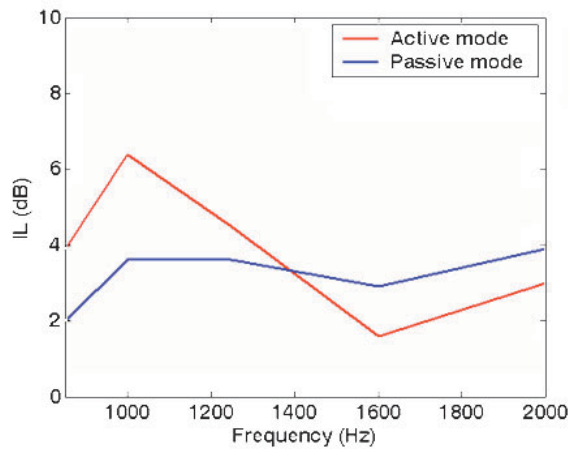


Figure 11. Insertion Loss measured in active and passive modes. The source is on the left. The Mach number is 0.15

7. COMPARISON WITH NUMERICAL SIMULATION

Numerical simulation used the PATRAN and ACTRAN software packages. PATRAN is a mechanical computer-aided engineering program used for design and post-processing. ACTRAN is a finite/infinite element program for modeling sound propagation,

transmission and absorption (see [8] for exhaustive details of the finite/infinite elements method). Precise 3D modeling of the experimental conditions was carried out only in the no-flow case. About 120,000 elements ($\lambda/3$ mesh: 0.046 m quadratic tetrahedral elements) were necessary to describe the finite element domain containing the whole duct. A homogeneous impedance condition was applied to the walls, in contrast to the experimental set-up where rigid separators inherent in each cell checked the whole surface (see Fig. 5). The impedance values were derived from measurements made in a Kundt tube. The real part of the specific impedance always remained close to 1, while the imaginary part depended on the operating mode, tending towards 0 in the active mode, and increasing from -3 at 850 Hz to -1 at 2 kHz in the passive mode. The sources were spherical point sources, located at the center of each source panel, as in the test bench. The pressure field at the antenna was calculated outside the finite element domain using infinite elements based on a multipole expansion. Calculation was carried out on an entire half-sphere, in order to obtain complete information on the radiated field. The geometrical model used for the duct and antenna is shown in Fig. 12.

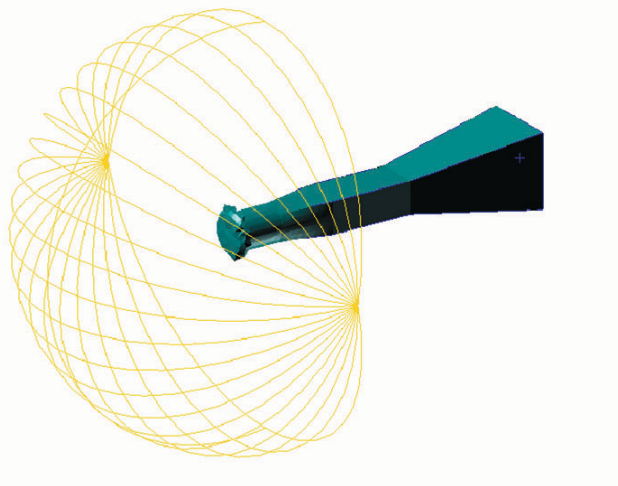


Figure 12. Duct and antenna model

Figures 13 and 14 illustrate the pressure fields obtained with the left-hand source, respectively for the rigid wall and then for the active and passive modes. All the diagrams are plotted on the same scale. The calculated pressure fields are shown first on the same surface as that measured, and then, in the last column, on the entire half-sphere. Experiments and simulations were in good agreement: the calculated directivity patterns reflected the measured ones overall, except for two cases: at 850 Hz in rigid mode, and at 1.25 kHz in all cases. At 850 Hz, the discrepancy may have come from the proximity between this frequency and the (1,1) mode of the rectangular duct cross-section. Besides, the hypothesis of point sources, which leads to theoretical results omitting some modes, was clearly not verified by the test rig.

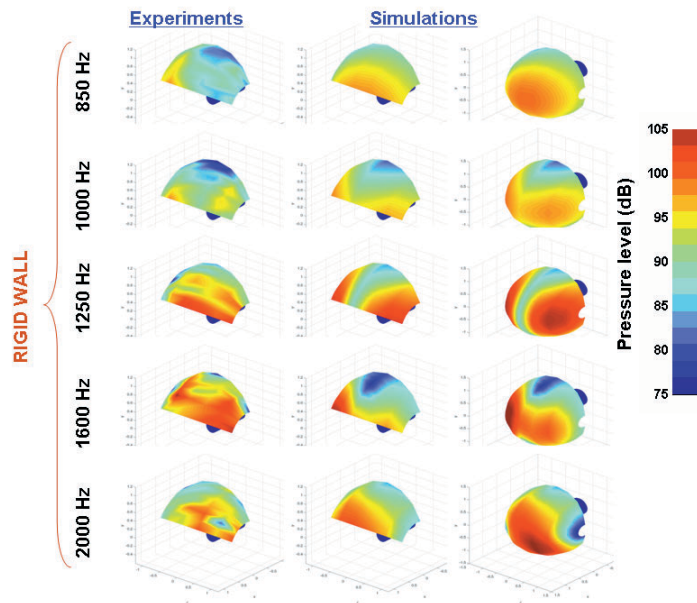


Figure 13. Pressure field measured and calculated for the source located on the left. Rigid wall case

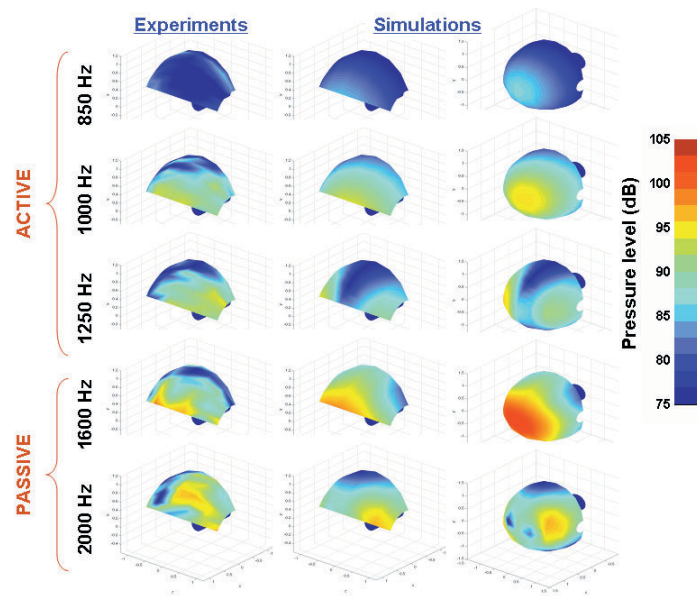


Figure 14. Pressure field measured and calculated for the source located on the left. Active and passive modes

Overall, however, simulation confirmed the interest of active control for the lowest frequencies, even if the sound reductions were greater than in the experiments. Insertion Loss was calculated and is plotted in Fig. 15 for the left-hand source. The trends were similar to the experimental behavior, with a cut-off between active and passive functioning located around 1.5 kHz - i.e., slightly higher than as measured experimentally.

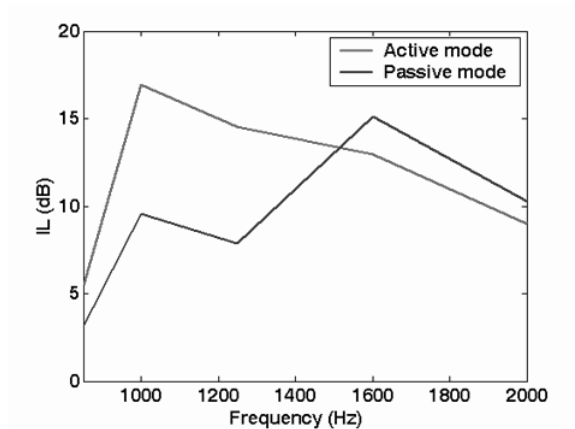


Figure 15. Insertion Loss calculated in active and passive modes. The source is on the left

8. CONCLUSIONS

Two hybrid active/passive panels were designed to provide noise reduction in flow-duct applications over a wide frequency range. Tests carried out in an anechoic wind tunnel showed the feasibility of such technology. The controller design was validated for about fifty cells: convergence was fully satisfactory during the tests and the signal was well controlled at each error microphone. This is a very interesting and promising result: the architecture of hybrid liners allows large absorbent surfaces to be developed, and active control was effective at a representative Mach number. Pressure-field measurements showed that active functioning was generally more effective at low frequencies (850 and 1 kHz) and passive functioning at frequencies above 1.25 kHz. The experimental conditions were precisely modeled by the ACTRAN aeroacoustics software package, confirming this pattern. Good overall reduction was obtained with the hybrid liner.

Simulations should be further developed, taking flow into account, particularly at high Mach numbers where the liner performance seems to decrease. Optimal impedance, defined as that which provides the greatest sound reduction, could thereby be determined. Precise implementation over a wide frequency bandwidth and for different flow velocities would probably involve developing a strategy for complete simultaneous control of both real and imaginary components.

ACKNOWLEDGMENTS

This research was partly carried out under a partnership between SNECMA, AIRBUS France, 01dB-METRAVIB and Ecole Centrale de Lyon, and was supported by the European Union under the SILENCE(R) project (GRD1-2000-25297).

REFERENCES

- [1] Furstoss, M., Thenail, D., Galland, M.A., Surface impedance control for sound absorption: direct and hybrid passive/active strategies, *Journal of Sound and Vibration*, 1997, 203(2), 219-236.
- [2] Sellen, N., Custa, M., Galland, M.A., 2006, Noise reduction in a flow duct: implementation of a hybrid passive/active solution, *Journal of Sound and Vibration*, In Press, Available online 21 June 2006.
- [3] Olson, H. F. and May, E. G., Electronic sound absorber, *Journal of the Acoustical Society of America*, 1953, 25, 1130-1136.
- [4] Tester, B.J., The propagation and attenuation of sound in lined ducts containing uniform or plug flow, *Journal of Sound and Vibration*, 1973, 28(2), 151-203.
- [5] Hilbrunner, O., Galland, M.A., Sellen, N., Perisse, J., Optimisation of a hybrid acoustic liner for noise reduction of engine aircraft nacelles, *Proceedings of ACTIVE 2002 - The 2002 International Symposium on Active Control of Sound and Vibration*, 1, Southampton, UK, 2002, 657-668,.
- [6] Elliott, S.J., Sutton, T.J., Rafaely, B. and Johnson, M., Design of feedback controllers using a feedforward approach, *Proceedings of ACTIVE 1995 - The 1995 International Symposium on Active Control of Sound and Vibration*, 1995, 561-572.
- [7] B. Mazeaud, B., Galland, M.A., Sellen, N., Design of an adaptive hybrid liner for flow duct applications, *10th AIAA/CEAS Aeroacoustics Conference, Manchester, UK*, 2004, AIAA Paper 2004-2852.
- [8] Astley, R.J., Macaulay, G.J., Coyette, J.P., and Cremers, L., Three-dimensional wave envelope elements of variable order for acoustic radiation and scattering. Part I: Formulation in the frequency domain, *Journal of the Acoustical Society of America*, 1998, 103(1), 49-63.